Identification of Modal Parameters of Classically Damped Linear Structures under Multi-Component Earthquake Loading

M. Mahmoudabadi [1], M. Ghafory-Ashtiany [2], and M. Hosseini [3]

1. Structural Earthquake Engineering, International Institute of Earthquake Engineering and Seismology (IIEES), Tehran, Iran, email: mahmoud@iiees.ac.ir
2. President, International Institute of Earthquake Engineering and Seismology (IIEES), Tehran, Iran
3. Structural Engineering Research Center, International Institute of Earthquake Engineering and Seismology (IIEES), Tehran, Iran

ABSTRACT: *A new method for the identification of dominant modal parameters (natural frequencies, damping ratios and participation factors) of classically damped linear structures using response to a multi-component earthquake is presented. If different components of the base acceleration of a structure are measured, the possibility of coupling between each of the six components of an earthquake and the measured absolute acceleration of the structure can be investigated. After introduction of the modal equations of motion of classically damped linear systems under multi-component earthquake, a newly proposed method for identification of the structural modal parameters is explained and, by application of the method to a model and on a real structure using artificial and real earthquake records, the accuracy of the method has been verified. The results of this verification indicate that the effect of the multi-input can be important for the identification of modal damping ratios and modal participation factors, and can improve compatibility between the recorded acceleration response and the calculated model response.*

Keywords: System identification; Modal parameters; Classical damping; Linear systems; Multi-component earthquake; Optimal parameters; Seismic response

1. Introduction

The main effort of structural dynamics is defining input loads, establishing analytical structural models, and developing suitable numerical schemes for the evaluation of a response. The applicability of analytical solutions is limited to the degree of realistic representation of the formulated mathematical models. A logical prelude to prediction of the dynamic response of a system is the determination of its dynamic properties, which can be made through the application of system identification theory. System identification is an inverse structural dynamics problem which involves determination of mathematical models and estimation of structural parameter values on the basis of measured responses of structures under known inputs or ambient vibration.

Many system identification techniques are classified as output-error methods. The system parameters are obtained by minimizing the discrepancy between recorded and theoretical responses of the system. The evaluated parameter is called an optimal estimate. The main problem in these techniques is that seismic response is usually only measured at a few locations in a structure. This limits the degree to which the dynamic properties of a system can be resolved. However, modal frequencies,

modal damping ratios and effective participation factors can be determined, with reasonable accuracy, for linear models on the basis of a single response measurement [1]. A generalized modal identification technique for non-linear systems was also proposed by Peng [2]. In short, insufficiency of response measurements makes a modal approach in system identification popular.

Beck [1] was one of the first to study structural system identification by determining the linear models of structures from seismic response data. He employed an output-error approach, in which optimal estimates of the model parameters were obtained by minimizing a selected measure-of-fit between the responses of the structure and the model. Because earthquake records are normally only available from a small number of locations in a structure, and because of the noise measurement, it was shown that it is necessary to estimate the parameters of the dominant modes in the records, rather than the stiffness and damping matrices. Beck also applied the modal minimization method to two multi-story building in the 1971 San Fernando earthquake. He obtained new information concerning the properties of higher modes of taller building and obtained more reliable estimates of the properties of the fundamental modes of both structures.

McVerry [3] has done work similar to Beck's for frequency domain. He developed a systematic frequency domain identification technique to determine optimal linear model parameters. In his method, the periods, damping and participation factors were estimated for the structural modes which were dominant in the measured response. He assumed that structures had a planar behavior which was the response in a given direction caused only by the component of the input in that direction. Identification was made by finding the values of the modal parameters which produce a least-squares match over a specified frequency range between the unsmoothed, complex-valued, finite Fourier transform of acceleration response recorded in the structure and that calculated for the model. It was possible to identify a single linear model for the entire response, or to approximate the nonlinear behavior exhibited by some structures with a series of models optimal for different segments of the response.

Li and Mau [4] used a multiple-input/multiple-output system identification procedure for the analysis of the seismic records. Their procedure was an extension of the least-square-output-error method applied to a classically damped linear second order system. The time varying behavior was modeled through a time window approach. The records of a 15-story reinforced concrete building in the Whittier earthquake were analyzed, and it was shown that the torsional response was significant and was caused by both the translational and the torsional motions at ground level.

Goal and Chopra [5] have developed a database on vibration properties (period and damping ratio of the first two longitudinal, transverse and torsional vibration modes) of buildings "measured" from their motions recorded during eight earthquakes in California (1971 San Fernando to 1994 Northridge earthquake). In their investigation, the natural vibration periods of 21 buildings were measured using the system identification method applied to the motions of buildings recorded during the earthquakes. They used the system identification toolbox of *MATLAB* software [6] for identification of modal frequencies and damping ratios.

Arici and Mosalam [7] used a multi-input/single-output system identification method for instrumented bridges. The recorded motions (actual response) of seven bridges in California during recent earthquakes were used in parametric and non-parametric system identification methods to obtain the modal frequencies and damping ratios of the bridges. They said that the excellent fit of the recorded motion in the time domain was obtained using parametric methods. They also used constructed linear filters for response prediction for three bridges and concluded that reasonable prediction results were obtained considering the limitations of the procedure.

In Iran, several studies have been performed for system identification of model and actual structures (buildings, concrete and earth dams, offshore oil platforms) using ambient and forced vibration methods. Aghakouchak and Memari [8] identified natural frequencies, mode shapes and modal damping of a six story building with an ambient and forced vibration test; the first study of this type in Iran. Memari, et al [9] performed an ambient vibration test on a 32-story building to determine its dynamic properties and fine tune the analytical modeling. The properties of interest from the test were frequencies, mode shapes and damping ratios for the first few modes. Ghafory-Ashtiany, et al and Kazem, et al [10-12] made extensive system identification and damage

assessment studies on a half-scale model of typical steel structures in Iran using forced vibration technique. Saberi-Haghighi, et al [13] proposed a procedure based on backpropagating feedforward neural network simulators and a genetic algorithm identifier for damage assessment of structures. They used the experiments data of the half-scale model mentioned above to investigate the performance of this proposed method in conjunction with real data. Ghafooripour and Aghakoochack [14] have applied ambient vibration test for system identification of an offshore oil platform in Persian Gulf. Mivehchi [15] evaluated dynamic characteristics and behavior of Saveh concrete arch dam using ambient vibration tests and of the Shahid Rajaie concrete dam using forced vibration and proposed an identification procedure with a minimum number of response measurements. Davoodi [16] performed a complete system identification on the Marun embankment dam ambient vibration measurements and from low-level loads such as wind, machinery movement, low level tectonic activities and water exit from the bottom outlet. He also performed force vibration and ambient vibration test on Masjid Solyman embankment dam. He identified natural frequencies, mode shapes and modal damping of the lower vibration modes of both dams from the results of these tests.

In addition to the identification of dynamic characteristics of different structures in Iran, several important buildings were instrumented by accelerographs to record their responses during an actual earthquake. In order to have a systematic approach to processing these seismic responses McVerry's method was adopted and is extended for a six-components earthquake for the general case. This extended method was verified using generated test data and then applied to measured earthquake responses obtained during Northridge earthquake.

2. Modal Equations of Motion of Classically Damped Linear Systems due to Six-Component Earthquake Loading

The governing equation of motion of an n degree of freedom linear system subjected to the base excitation is expressed as:

$$M\ddot{V}(t)+C\dot{V}(t)+KV(t)=-MRE(t) \tag{1}$$

in which M, C and K are the mass matrix, damping matrix, and stiffness matrix of the system, respectively; $\ddot{V}(t), \dot{V}(t)$ and $V(t)$ are the relative acceleration, velocity and displacement vector of the system, respectively; R, is the influence coefficients matrix of earthquake input; and $E(t)$ is the ground acceleration vector consisting of six components as follows:

$$E(t)=\begin{Bmatrix} \ddot{x}_g(t) \\ \ddot{y}_g(t) \\ \ddot{z}_g(t) \\ \ddot{\theta}_{gx}(t) \\ \ddot{\theta}_{gy}(t) \\ \ddot{\theta}_{gz}(t) \end{Bmatrix} \equiv \begin{Bmatrix} \ddot{x}_1(t) \\ \ddot{x}_2(t) \\ \ddot{x}_3(t) \\ \ddot{x}_4(t) \\ \ddot{x}_5(t) \\ \ddot{x}_6(t) \end{Bmatrix} \tag{2}$$

By means of the normal mode shapes matrix (Φ) and with the classical damping assumption, Eq. (1) transforms to an n decoupled differential equation as follows:

$$\ddot{y}_r(t)+2\zeta_r\omega_r\dot{y}_r(t)+\omega_r^2 y_r(t)= -\sum_{j=1}^{6} p_{jr}\ddot{x}_j(t)\ ,\ r=1,\ldots,n \tag{3}$$

where coefficients, p_{jr}, is defined as:

$$p_{jr}=\frac{\varphi_r^T M r_j}{\varphi_r^T M \varphi_j},\quad j=1,....,6 \tag{4}$$

in which φ_r is the r^{th} mode shape vector and r_j is the influence vector of earthquake in the j direction (j^{th} column of R). Considering that φ_{pri} is the i^{th} component of r^{th} mode shape at position p of the structure in the x direction and that every joint in the structure has six mode shape components in six principle directions, the pre-multiplication of Eq. (3) in φ_{pri} results in:

$$\ddot{x}_{pr}(t)+a_r\dot{x}_{pr}(t)+b_r x_{pr}(t)=-\sum_{j=1}^{6} c_{ijpr}\ddot{x}_j(t)\ ,\ r=1,\ldots,n \tag{5}$$

in which:

$$x_{prt}(t)=\varphi_{pri}y(t),\ a_r=2\zeta_r\omega_r\ ,\ b_r=\omega_r^2,$$
$$c_{ijpr}=\varphi_{pri}\frac{\varphi_r^T M r_j}{\varphi_r^T M \varphi_r}\ ,\quad j=1,\ldots,6 \tag{6}$$

Similar equation can be developed for other directions. Eq. (5) is the modal equation of motion for a system subjected to six components earthquake (three translational and three rotational). In this general case, there is a modal participation factor, for each earthquake component. The first index of

c_{ijpr}, i, addresses the direction in which absolute acceleration of structure is measured. The second index, j, indicates the direction of the earthquake component. The third index, p indicates the position of the measured acceleration of the structure and the fourth index, r, addresses the vibration mode number. It is assumed that the measured quantities are ground acceleration components $\ddot{x}_j(t)$, j = 1, ..., 6 in the x, y, z, r_x, r_y and r_z directions and the absolute acceleration response at one or more positions in the structure.

The modal equations can be transformed into frequency domain via Fourier transform. Although the interval of integration of the transform is semi-infinite in practice, this transform will be both finite and discrete as found by use of the Discrete Fourier Transform (*DFT*). The Finite Fourier Transform $F(\omega, T)$ of $f(t)$ over a record length T is defined as

$$F(\omega,T)=\int_0^T f(t)e^{-i\omega t}dt, \quad i=\sqrt{-1} \tag{7}$$

assuming that the finite Fourier transform of the ground acceleration components $\ddot{x}_j(t)$, j = 1, ..., 6 over the duration of T are $X_j(\omega,T)$, j = 1, ..., 6. The *DFT* algorithm produces the complex-valued transforms at N equally-spaced frequencies ω_n from 2 N equally spaced samples of a record of length T where

$$\omega_n = nD\omega = \frac{2\pi n}{T}, \quad n=0,1,...,N-1 \tag{8}$$

The finite Fourier transform of absolute acceleration $\ddot{x}_p(t)+\ddot{x}_g(t)$; $\overline{A}_p(\omega,T)$ using the McVerry [3] approach becomes

$$\begin{aligned}\overline{A}_p(\omega,T) = {} & X_1(\omega,T)+\omega^2\sum_{j=1}^{6}\sum_{r=1}^{Nm}c_{xjpr}H_r(\omega)X_j(\omega,T)+\\ & \sum_{r=1}^{Nm}\left[1+\omega^2 H_r(\omega)\right]v_{pr}+\\ & \sum_{r=1}^{Nm}\left[i\omega+\omega^2(i\omega+a_r)H_r(\omega)\right]d_{pr}, \quad i=\sqrt{-1}\end{aligned} \tag{9}$$

where $H_r(\omega)$ is the r^{th} mode transfer function which is defined as

$$H_r(\omega)=\frac{1}{(b_r-\omega^2)+i\,a_r\omega}, \qquad i=\sqrt{-1} \tag{10}$$

and v_{pr} and d_{pr} are the differences in the modal velocities and displacements between the beginning and end of the record segment of duration T:

$$v_{pr}=\dot{x}_{pr}(T)-\dot{x}_{pr}(0) \tag{11}$$

$$d_{pr}=x_{pr}(T)-x_{pr}(0) \tag{12}$$

Eq. (9) represents the response of the model of the system for which the parameters a_r, b_r, c_{xjpr} ($j = x, \ldots, r_z$), v_{pr} and d_{pr} are to be identified for Nm modes. It must be noted that the existence of the finite Fourier transform of the x direction "$X_1(\omega, T)$" in the beginning of Eq. (9) is for transformation of the relative acceleration to the absolute acceleration. For the other directions, the corresponding finite Fourier transform is added to the first of Eq. (9).

3. The Error Criteria

The system identification process was performed by selecting parameters to obtain a least-squares fit of the model response (Eq. (9)), to the transform of the measured response acceleration over a specified frequency band. That is:

$$J=\sum_{l=l_{min}}^{l_{max}}\left|A(lD\omega,T)-\overline{A}_p(lD\omega,T)\right|^2 \tag{13}$$

with respect to the parameters a_r, b_r, c_{xjpr} (j=x, ..., r_z), v_{pr} and d_{pr} (r = 1,..., Nm), of the Nm modes of the model. In Eq. (13), A is the discrete finite Fourier transform of the measured response acceleration, $\Delta\omega=2\pi/T$ and $0 \le l_{min} < l_{max} \le N-1$.

The normalized error E is defined as the mean square error divided by the mean square response taken over the same frequency band and for the same segment of record:

$$E=\frac{\sum_{l=l_{min}}^{l_{max}}\left|A(lD\omega,T)-\overline{A}_p(lD\omega,T)\right|^2}{\sum_{l=l_{min}}^{l_{max}}\left|A(lD\omega,T)\right|^2} \tag{14}$$

A similar normalized time-domain error criterion has been used by Werner, et al [17] and defined as

$$E'=\frac{\sum_{i=1}^{N}(y_i-\overline{y}_i)^2}{\sum_{i=1}^{N}(y_i)^2} \tag{15}$$

where y_i and $\overline{y}_i$ are the actual recording from the structure and the simulated model output, respectively. Arici and Mosalam [7] have claimed that a value of E' less than 0.1 corresponds to an excellent model. An E' of 0.1-0.5 corresponds to an adequate

model and time history fits where E' is greater than 0.5 are poor and the corresponding results should be disregarded. In Parseval's theorem, the error criterion in Eqs. (14) and (15) are identical if all the *DFT* frequency points are used in the identification process.

It is an important feature of the approach that the data used for the identification be in the form of the real and imaginary parts of the unsmoothed Fast Fourier transforms of the untapered segment of duration T of the measured ground acceleration, and the corresponding segment of the recorded response. Any smoothing of the *FFT* and tapering of the initial and final portions of the acceleration records introduces bias into the estimates of the parameters. Such untapered, unsmoothed data typically produce extremely poor transfer functions for parameter estimation using common resonant amplification and half-power methods. However, it will be seen that the parameter values obtained from the present approach are accurate.

4. The Identification Algorithm

The least-squares minimization of J in Eq. (13) is performed using an iterative Gauss-Newton type approach to solve the non-linear algebraic equations resulting from setting the partial derivatives of J to zero. The algorithm takes advantage of the linearity of the equations with respect to modal participation factors and modal displacement and velocity differences. The technique ensures that error is reduced at each iteration. Consider

$$\begin{aligned} \mathbf{?}^T = (&a_1,\ldots,a_{Nm},b_1,..,b_{Nm},c_{xx1},\ldots,c_{xxNm},\ldots,c_{xr_z1},\ldots,\\ &c_{xr_zNm},v_1,\ldots v_{Nm},d_1,\ldots,d_{Nm}) \end{aligned} \tag{16}$$

where, for simplicity, the subscript p (denoting dependence on position) is dropped. For a least square local minimum, partial derivatives J to the parameters of γ:

$$\frac{\partial J}{\partial \mathbf{?}} = 0 \tag{17}$$

and the second derivative matrix

$$\nabla_{?}(\nabla_{?}J) = \left[\frac{\partial^2 J}{\partial ?_i ?_j}\right],\ i = 1,\ldots,10Nm,\ j = 1,\ldots,10Nm \tag{18}$$

must be positive definite. The individual equations of Eq. (17) take the form

$$\begin{aligned} \frac{\partial J}{\partial \gamma_i} = -2 \sum_{l=l_{min}}^{l_{max}} \times \\ \left\{ Re\left[A(lD\omega,T) - \overline{A}(lD\omega,T)\right] Re\left[\frac{\partial \overline{A}(lD\omega,T)}{\partial ?_i}\right] + \right. \\ \left. Im\left[A(lD\omega,T) - \overline{A}(lD\omega,T)\right] Im\left[\frac{\partial \overline{A}(lD\omega,T)}{\partial ?_i}\right] \right\} = 0 \end{aligned} \tag{19}$$

The set of equations

$$\frac{\partial J}{\partial \mathrm{a}} = 0, \qquad \frac{\partial J}{\partial \mathrm{b}} = 0 \tag{20}$$

are non-linear with respect to all parameters in γ. However, the equations

$$\frac{\partial J}{\partial \mathrm{c}_{xx}} = 0\ ,\ldots,\quad \frac{\partial J}{\partial \mathrm{c}_{xr_z}} = 0,\quad \frac{\partial J}{\partial \mathrm{v}} = 0,\quad \frac{\partial J}{\partial \mathrm{d}} = 0 \tag{21}$$

are linear in the parameters $c_{xj}(j = x, \ldots, r_z)$, v and d, although non-linear in a and b. This condition suggests a two-part iterative algorithm that takes advantage of the linearity of Eq. (21) with respect to $c_{xj}(j = x, \ldots, r_z)$, v and d. First, initial estimates are chosen for all parameters. Then nonlinear Eq. (20) is solved approximately using a modified Gauss-Newton method to produce new values of a and b. The linear Eq. (21) is then solved exactly for $c_{xj}(j = x, \ldots, r_z)$, v and d corresponding to the latest values of a and b. The process is repeated until a selected convergence criterion is satisfied. The special case of the algorithm for one earthquake component is given by McVerry [3].

5. Application and Verification of the Proposed Identification Algorithm

A computer program based on *MATLAB* was developed for the proposed algorithm [18-21]. The performance of the method can be illustrated by the results of identifications applied to a model structure, see Figure (1), and to an actual structure subjected to real earthquake input (a 10-story concrete building in Burbank subjected to the Northridge earthquake, Figures (10) and (11)).

5.1. Six-Degrees-of-Freedom Model Structure

For the verification test of the identification algorithm, the parameters of a six-degrees-of-freedom structure were estimated from simulated data generated for its response to a six-component artificial earthquake. As shown in Figure (1), this structure is composed

of a rigid horizontal rectangle plate a with size $a \times b$ and uniform mass distribution (total mass is equal m) which is supported by a massless column with a height h. The degrees of freedom of structure are assumed at the center of the mass of the plate and, according to these degrees of freedom, mass and stiffness matrices of the structure are:

$$M = \begin{bmatrix} m & 0 & 0 & 0 & 0 & 0 \\ 0 & m & 0 & 0 & 0 & 0 \\ 0 & 0 & m & 0 & 0 & 0 \\ 0 & 0 & 0 & \frac{mb^2}{12} & 0 & 0 \\ 0 & 0 & 0 & 0 & \frac{ma^2}{12} & 0 \\ 0 & 0 & 0 & 0 & 0 & \frac{m(a^2+b^2)}{12} \end{bmatrix} \quad (22)$$

$$K = \begin{bmatrix} \frac{12EI_y}{h^3} & 0 & 0 & 0 & \frac{-6EI_y}{h^2} & \frac{6EbI_y}{h^3} \\ 0 & \frac{12EI_x}{h^3} & 0 & \frac{6EI_x}{h^2} & 0 & \frac{-6EaI_x}{h^3} \\ 0 & 0 & \frac{EA}{h} & \frac{-EbA}{2h} & \frac{EaA}{2h} & 0 \\ 0 & \frac{6EI_x}{h^2} & \frac{-EbA}{2h} & \frac{Eb^2A}{4h}+\frac{4EI_x}{h} & \frac{-EAab}{4h} & \frac{-3EaI_x}{h^2} \\ \frac{-6EI_y}{h^2} & 0 & \frac{EaA}{2h} & \frac{-EAab}{4h} & \frac{Ea^2A}{4h}+\frac{4EI_y}{h} & \frac{-3EbI_y}{h^2} \\ \frac{6EbI_y}{h^3} & \frac{-6EaI_x}{h^3} & 0 & \frac{-3EaI_x}{h^2} & \frac{-3EbI_y}{h^2} & \frac{3Ea^2I_x}{h^3}+\frac{3Eb^2I_y}{h^3}+\frac{GJ}{h} \end{bmatrix} \quad (23)$$

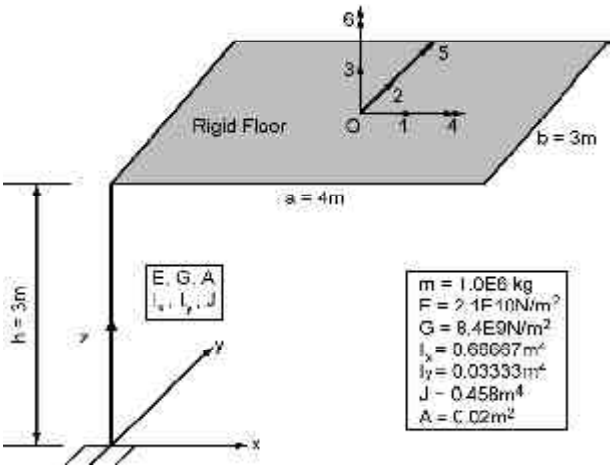

Figure 1. The six-degrees-of-freedom model structure used for the verification test of the proposed identification algorithm.

Natural frequencies and mode shapes of the system are presented in Tables (1) and (2) showing the participation factors of the x-direction, computed using Eq. (6). The damping ratio is assumed to the 0.02 for all modes.

Six uncorrelated, stationary, artificial random-generated base acceleration records, as in Figure (2), were applied to the six principle directions of the six degrees of freedom structure. The frequency content of these records is shown in Figure (3). Time history response of the structure computed using recurrence formulas [22] with the time steps of 0.005 seconds are shown in Figure (4). The

Table 1. Natural frequencies and mode shapes of six-degrees-of-freedom model.

Mode No.	1	2	3	4	5	6
Frequency (Hz)	0.8136	1.7641	2.8549	5.5400	9.4968	32.1310
Mode Shapes (φ_i)	-0.5330	0.6046	0.4601	-0.3597	0.0965	-0.0042
	0.0271	-0.5542	0.6032	-0.2918	-0.3258	0.3702
	0.7672	0.4527	0.4244	0.1507	-0.0607	-0.0046
	0.0062	0.0406	-0.0195	0.2140	0.7091	0.8847
	-0.3073	0.0027	0.2609	0.7372	-0.2100	-0.0022
	0.0182	-0.2412	0.2714	0.0430	0.4621	-0.3639

Table 2. x-direction participation factors of six-degrees-of-freedom structure.

Mode No.	c_{xx}	c_{xy}	c_{xz}	c_{xr_x}	c_{xr_y}	c_{xr_z}
1	0.2841	-1.444×10^{-2}	-0.4089	-2.496×10^{-3}	0.2184	-2.017×10^{-2}
2	0.3655	-0.3351	0.2737	1.839×10^{-2}	2.176×10^{-3}	-0.3038
3	**0.2117**	**0.2775**	**0.1953**	$\mathbf{-6.728\times10^{-3}}$	**0.1600**	**0.2601**
4	0.1294	0.1050	-5.420×10^{-2}	-5.774×10^{-2}	-0.3536	-3.223×10^{-2}
5	9.318×10^{-3}	-3.145×10^{-2}	-5.862×10^{-3}	5.134×10^{-2}	-2.703×10^{-2}	9.294×10^{-2}
6	1.742×10^{-5}	-1.545×10^{-3}	1.915×10^{-5}	-2.769×10^{-3}	1.223×10^{-5}	3.164×10^{-3}

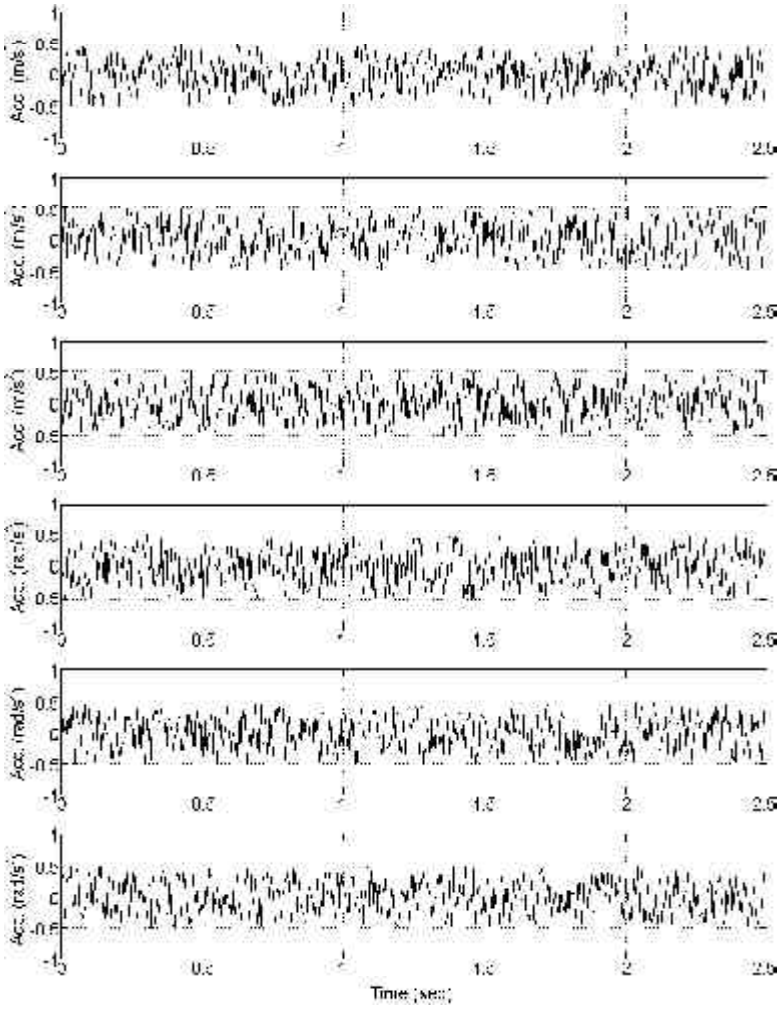

Figure 2. Base acceleration records applied to a six-degrees-of-freedom structure in the six principle directions *x, y, z,* r_x, r_y, and r_z from top to bottom, respectively.

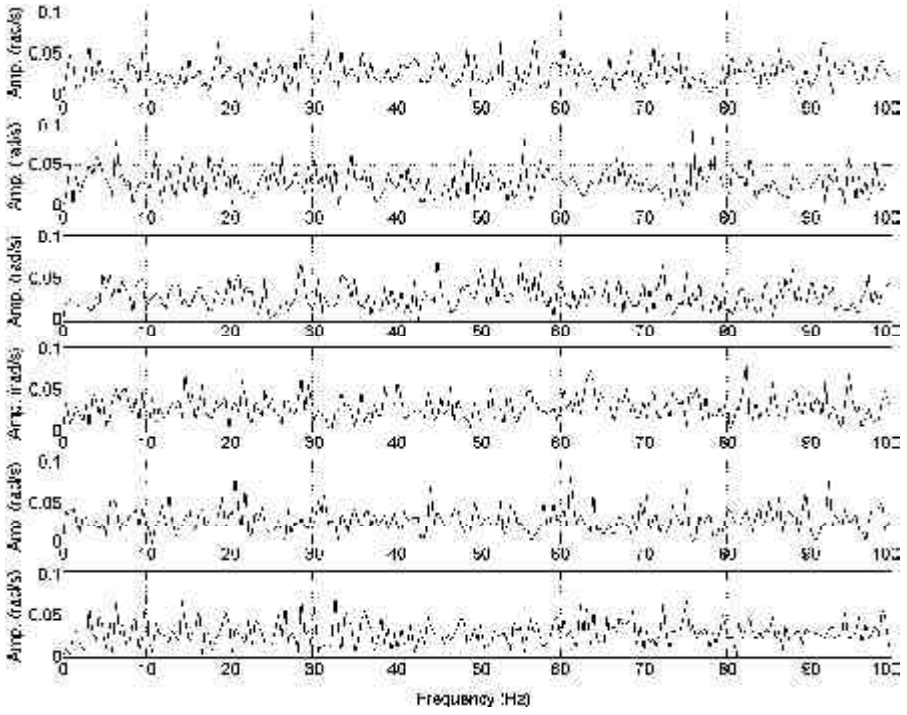

Figure 3. Frequency content of base acceleration records applied to a six-degrees-of-freedom structure in the six principle directions *x, y, z,* r_x, r_y, and r_z from top to bottom, respectively.

corresponding frequency content of the response is shown in Figure (5). For simplicity and as an example, only the identification of parameters of the third mode is shown, since its base acceleration records for the five direction x, y, z, r_y and r_z have considerable participation in the response of the structure in x

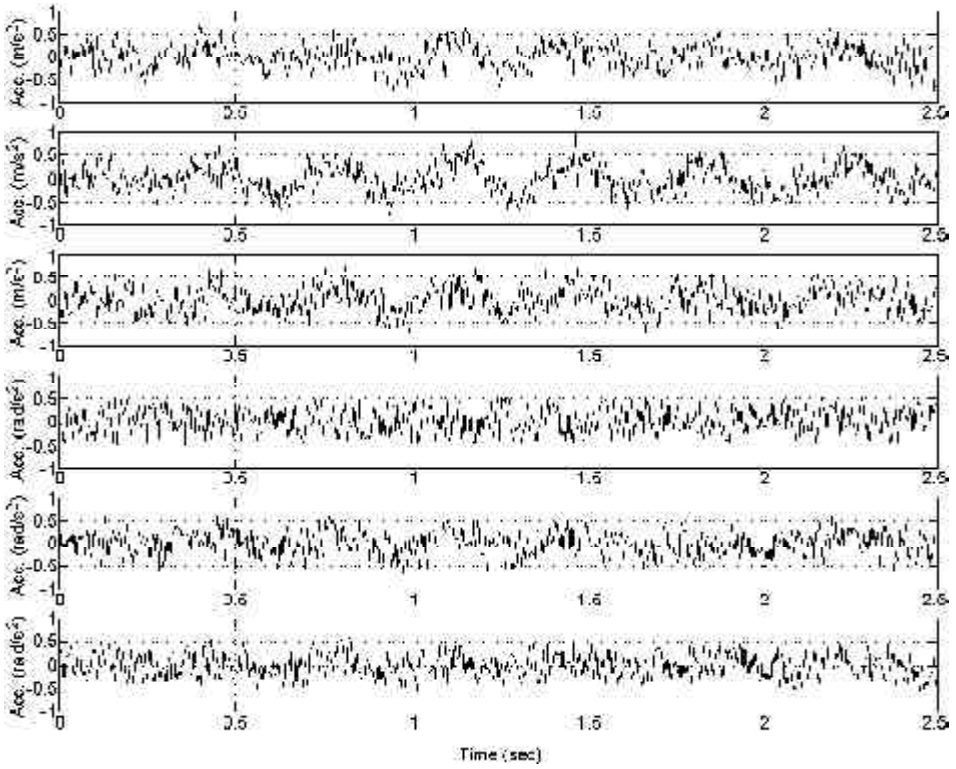

Figure 4. Response acceleration records of a six-degrees-of-freedom structure in principle directions x, y, z, r_x, r_y, and r_z from top to bottom, respectively (only effect of third mode is included).

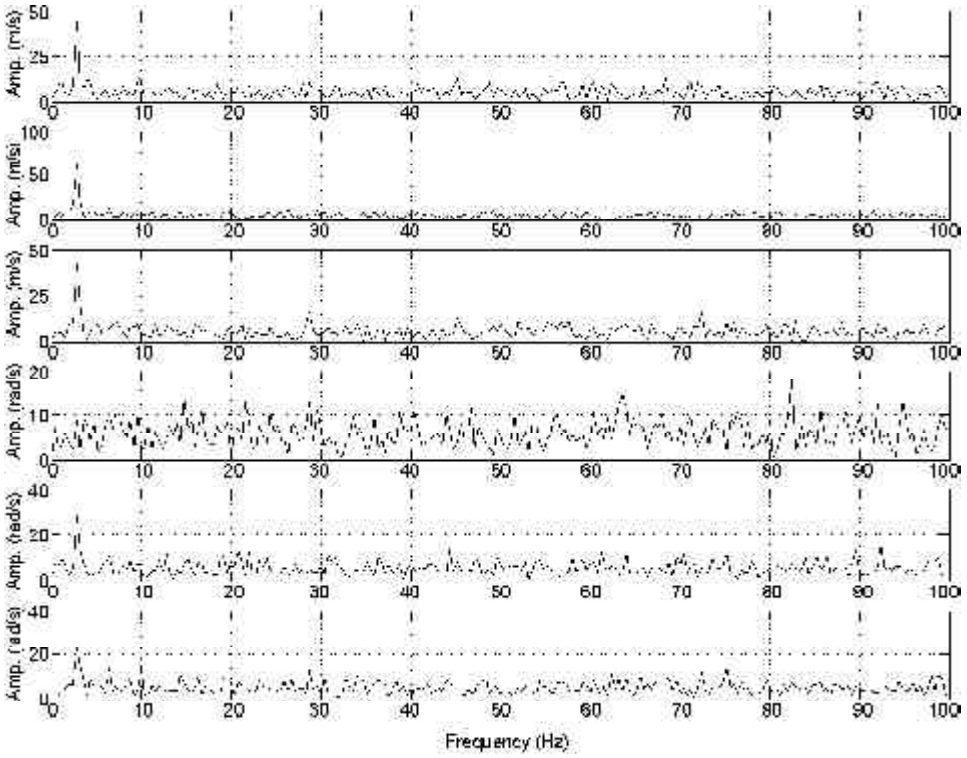

Figure 5. Frequency content of response acceleration records of a six-degrees-of- freedom structure in principle directions x, y, z, r_x, r_y, and r_z from top to bottom, respectively (only effect of third mode is included).

direction. The identification of the other parameters is given in [23].

In order to show the effect of different base acceleration components on the estimates of the modal parameters, the identification of parameters proceeds thus:

1. Assuming that the absolute acceleration of structure in the *x* direction results only from *x* direction acceleration, the modal parameters were identified. The results are presented in the first row of Table (3).

Table 3. Results of modal parameters identification of the third mode of six-degrees-of-freedom model for different number of components of an artificial excitation.

No. of Eq. Comp.	Parameter Condition	f (Hz)	ζ (%)	c_{xx}	c_{xy}	c_{xx}	c_{xr_x}	c_{xr_y}	c_{xr_z}	Normalized Error
1	Exact Values	2.8549	2.00	0.2117	0.2775	0.1953	-6.728E-3	0.1600	0.2601	0.2363
	Identified Values	2.8257	1.2317	0.2203	-----	------	------	-----	------	
	Error (%)	-1.02	-38.42	4.06	-----	------	------	-----	------	
2	Identified Values	2.8747	0.0151	0.1823	0.2830	------	------	-----	------	0.12939
	Error (%)	0.70	-99.25	-13.89	1.98	------	------	-----	------	
3	Identified Values	2.8958	0.0803	0.1641	0.2802	0.1804	------	-----	------	0.095007
	Error(%)	1.43	-95.99	-22.48	0.97	-7.63	------	-----	------	
4	Identified Values	2.8964	0.0689	0.1638	0.2803	0.1803	-4.322E-3	-----	------	0.094986
	Error (%)	1.45	-96.56	-22.63	1.01	-7.68	-35.76	-----	------	
5	Identified Values	2.9038	0.8212	0.1788	0.2789	0.1763	-1.691E-3	0.1406	------	0.074224
	Error (%)	1.71	-58.94	-15.54	0.50	-9.73	-125.13	-12.11	------	
6	Identified Values	2.8560	1.9704	0.2102	0.2781	0.1956	-7.850E-3	0.1595	0.2594	8.819E-5
	Error (%)	0.04	-1.48	-0.71	0.22	0.15	14.29	-0.31	-0.27	

2. Assuming that the absolute acceleration of the structure in the *x* direction results from *x* and *y* direction base accelerations, the corresponding modal parameters were identified and compared with their exact values as shown in the second row of Table (3).
3. The above steps were repeated until all six component base accelerations were included in the identification process. Their corresponding results are given in the subsequent rows of Table (3).

In the single-input/single-output case (first row of Table (3)), the value of normalized error is equal to 0.2363 and with the addition of other earthquake components in each step, the value of normalized error gradually decreases and, finally, in the six components input case, the value of normalized error become very small and reaches to a negligible value of 8.819*E*-5.

With accurate consideration of Table (3), one can observe that frequency parameter has minimum value of the identification error, while the damping ratio parameter has maximum value of the identification error, almost in all of the cases. Also, the frequency parameter has a minimum variation in the process of identification while the damping ratio parameter has a maximum variation. Thus, according to this example, if all earthquake components are not included in the identification process, considerable identification error will occur in the damping ratio.

Since the base acceleration records applied to the 6*DOF* model were artificial and bear no resemblance to earthquake ground motion, it was decided to apply the base acceleration records of a ten-story concrete building (see section 5.2) to the 6*DOF* model. Figure (6) shows the time histories of these base acceleration and Figure (7) shows the corresponding frequency content of the base acceleration records.

Accelerograms of channels 16, 14 and 15 were applied in the *x*, *y* and *z* directions respectively at the base level of the model. The torsional accelerogram computed by means of parallel channels 1 and 13 also was considered as torsional base acceleration about the *z* axis, see Figure (11). As in previous case, the response of the 6*DOF* model was computed using recurrence formula. Time histories of the model response in six principle directions are shown in Figure (8) and their corresponding frequency contents are presented in Figure (9). Each accelerogram has 3000 points sampled at 0.02 seconds. Contrary to the previous case, the total modes effects were considered in the computation of the model response.

Identification of modal parameters in the *x* direction was performed as in the previous case. In this way, it was first assumed that the response of the 6*DOF* model in the *x* direction is resulted only

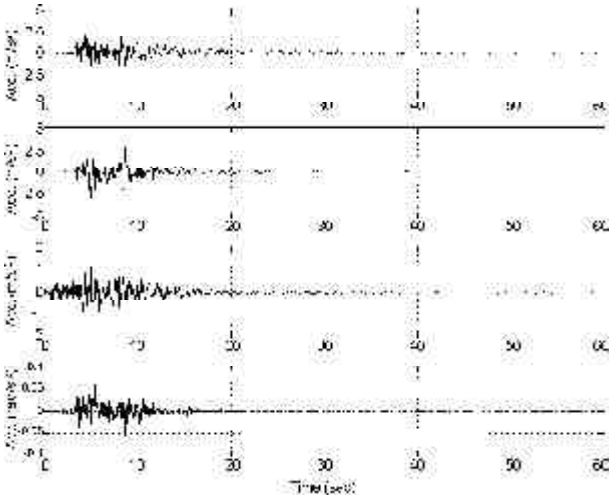

Figure 6. Base acceleration records applied to a six-degrees-of-freedom structure in the four principle directions *x, y, z,* and r_z from top to bottom, respectively.

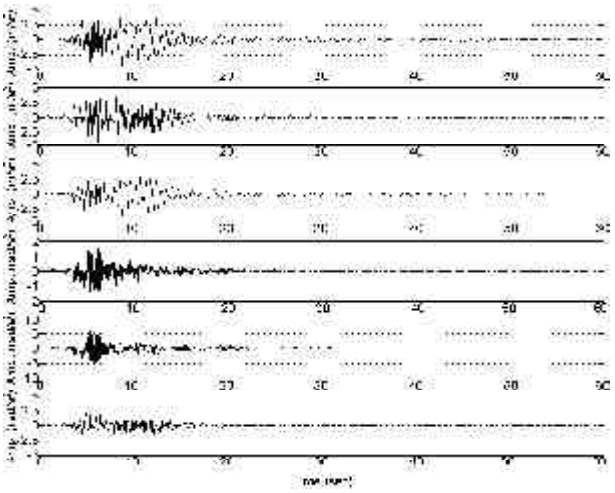

Figure 8. Response acceleration records of a six-degrees-of-freedom structure in principle directions *x, y, z,* r_x, r_y, and r_z from top to bottom, respectively.

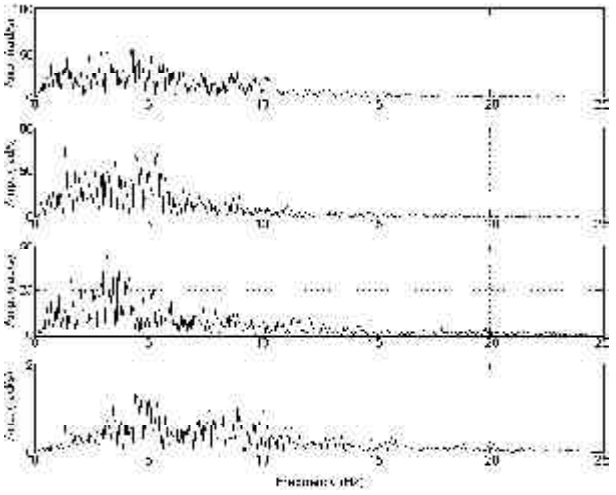

Figure 7. Frequency content of base acceleration records applied to a six-degrees-of-freedom structure in the four principle directions *x, y, z,* and r_z from top to bottom, respectively.

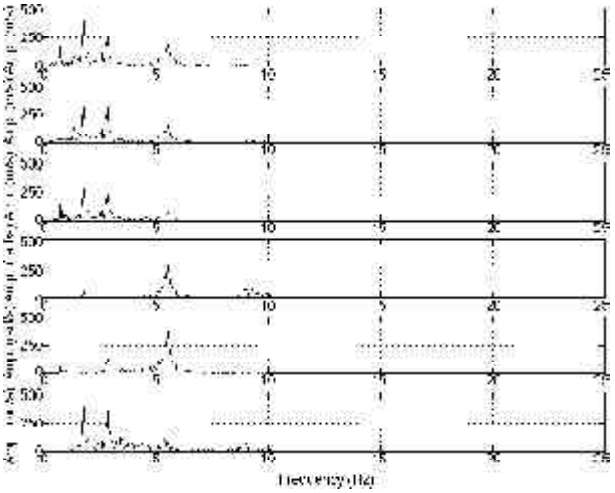

Figure 9. Frequency content of response acceleration records of a six-degrees-of- freedom structure in principle directions *x, y, z,* r_x, r_y, and r_z from top to bottom, respectively.

from the *x* direction base acceleration and the corresponding modal parameters are identified. Then, in the other directions, base acceleration components were included and modal parameters were identified. For briefness, only the results of identification of the third mode parameters are given in Table (4). The identification of the other parameters is given in Ref. [23].

It is observed in Table (4) that, with artificial excitation by including of more components of a real earthquake, the normalized error (a match criterion between the recorded acceleration response and calculated model response) decreases and the precision of identification of modal parameters increases.

The following conclusions can be obtained from Tables (3) and (4):

1. Error of identification of third modal frequency in all cases is negligible and including different components of an earthquake in the identification process has little effect on the identification of this modal frequency.
2. Contrary to modal frequency, identification of the third modal damping ratio and third modal participation factors are sensitive to the number of base acceleration components and, by ignoring the effect of different base acceleration components in the identification of modal parameters, relatively large errors can occur.

Table 4. Results of modal parameters identification of the third mode of a six-degrees-of-freedom model for different number of components of a real earthquake.

No. of Eq. Comp.	Parameter Condition	f (Hz)	ζ (%)	c_{xx}	c_{xy}	c_{xx}	c_{xr_z}	Normalized Error
	Exact Values	2.8549	2.00	0.2117	0.2775	0.1953	0.2601	
1	Identified Values	2.8317	2.2929	0.2330	------	------	------	0.353
	Error (%)	-0.81	14.65	10.06	------	------	------	
2	Identified Values	2.8519	1.8292	0.2704	0.2490	------	------	0.058894
	Error (%)	-0.11	-8.54	-27.73	-10.27	------	------	
3	Identified Values	2.8549	1.9910	0.2103	0.2738	0.1924	------	2.6036E-5
	Error (%)	0.00	-0.45	-0.66	-1.33	-1.48	------	
4	Identified Values	2.8548	1.9999	0.2095	0.2746	0.1931	0.2525	2.1029E-7
	Error (%)	-0.004	-0.005	-1.04	-1.05	-1.13	-2.92	

The measurement of all six components of an earthquake is difficalt since the rocking components of ground motion are seldom measured. Hence, to provide a clearer indication of the importance of torsional input without the complication of including all the other inputs, it was decided to bring in results which directly compare to the modal parameters estimation using one input (x direction) and two inputs (x and r_z directions) in Table (5), for both artificial excitation and real base acceleration. It can be observed in Table (5), that for both cases, by including the torsional base acceleration in the identification process, the match between the simulated acceleration response and the calculated model response improves considerably. In this way, normalized error decreases 27.66% and 14.64% respectively in comparison to one input excitation for artificial excitation and real base acceleration. However, this effect is less for real base acceleration, which may be attributed to lower amplitude of real torsional base acceleration relative to real translational base acceleration, regardless of their units, see Figures (6) and (7).

From Table (5) it can be understood that, by including the torsional component of base acceleration for artificial excitation, the error of identification of modal frequency is slightly increased, but the error of identification of modal damping ratio decreases considerably. This is opposite for real base accelerations. Also in the Table (5) there is an enormous error of identification of c_{xr_z} relative to the other modal parameters in the real base acceleration case. This may arise from the relatively small amplitude of torsional excitation in comparison with other translational base acceleration components as mentioned previously.

A real case will be considered in the next section and it will be shown that the participation of the torsional base acceleration about z axis plays an effective role in more precisely identifying the first mode damping ratio parameter of a nominal symmetric building.

Table 5. Results of modal parameters identification of the third mode of six-degrees-of-freedom model for the x direction and x with r_z direction components of an artificial excitation and a real earthquake.

Type of Base Accelerations	System Input	System Output	Parameter Condition	f (Hz)	ζ (%)	c_{xx}	c_{xr_z}	Normalized Error
Artificial Records	Base Acceleration in x direction	Absolute Acceleration in x direction	Exact Values	2.8549	2.00	0.2117	0.2601	0.2363
			Identified Values	2.8257	1.2317	0.2203	------	
			Error (%)	-1.02	-38.42	4.06	------	
	Base Acceleration in x and r_z direction	Absolute Acceleration in x direction	Identified Values	2.7714	1.6488	0.2460	0.2458	0.17095
			Error (%)	-2.92	-17.56	16.20	-5.50	
Earthquake Records	Base Acceleration in x direction	Absolute Acceleration in x direction	Identified Values	2.8317	2.2929	0.2330	------	0.353
			Error (%)	-0.81	14.65	10.06	------	
	Base Acceleration in x and r_z direction	Absolute Acceleration in x direction	Identified Values	2.8570	1.3762	0.1722	-3.5628	0.30133
			Error (%)	0.074	-31.19	-18.66	-1470	

5.2. Identification of Modal Parameters of a 10-Story Concrete Building in Burbank

The ten-story concrete building under study, as shown in Figure (10), was designed and constructed in 1974. The lateral load resisting system consists of precast concrete shear walls in both directions [24]. The plan and elevation of the building and the location of sensors are shown in Figure (11). Figure (12) shows the time histories of the recorded response of the building during the Northridge earthquake at the sensors locations. This earthquake data has been used to check the Spline function technique for reconstruction of seismic responses [25].

The largest peak horizontal acceleration recorded at the base (Channel 1, *N-S*) was 0.34*g*, and at the roof (Channel 2, *N-S*) was 0.77*g*. No sign of structural damage was observed during the inspections; however, only minor damage to the nonstructural equipment on the roof was observed [24]. For the identification of the modal parameters of this

Figure 10. General view of 10-story residential building in Burbank [24].

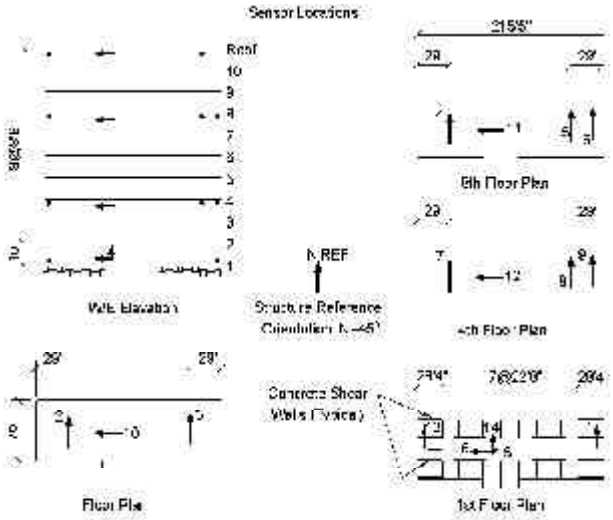

Figure 11. Plan and elevation of 10-story building in Burbank and location of the sensors [24].

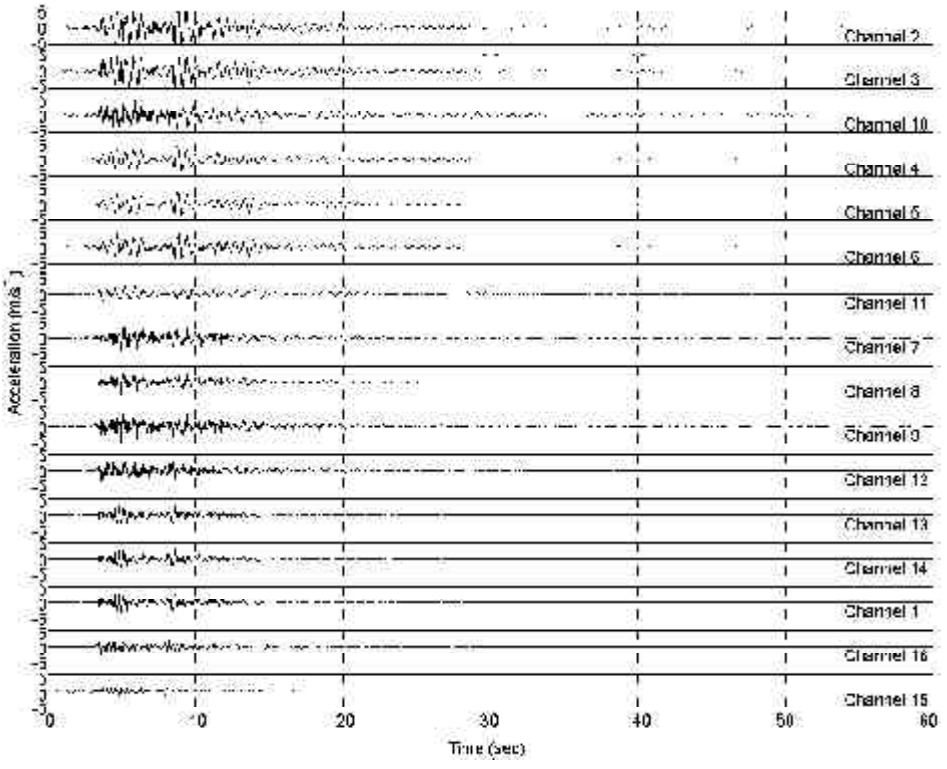

Figure 12. Time histories of the recorded response of a 10-story building during Northridge earthquake at the location of sensors [24].

building, a step-by-step procedure (see Section 5.1) was adopted as follows:

1. It was assumed that the recorded acceleration in the *N-S* or *E-W* direction of the building resulted only from base acceleration in the corresponding direction.
2. It was assumed that the two horizontal base accelerations can be effected in the recorded acceleration in the building.
3. It was assumed that in addition to the two horizontal base accelerations, vertical base acceleration can be effected in the recorded response of the building.
4. The rotational base acceleration about the *z* axis, with rigid base assumption and by means of two parallel sensors (Channels 1 and 13) was computed and this component of the earthquake participated in the identification of the modal parameters of the building.

Tables (6) through (9), show the results of the identification processes. It is noted that the direction of the *x*-axis coincides with *E-W* direction of the *y*-axis with the *N-S* direction and that of the *z*-axis is vertical. In order to better understand the variations of different modal parameters, the variation of normalized error, first and second modal

Table 6. Results of modal parameters identification of a 10-story building in Burbank for one component of an earthquake.

System Input	System Output	Direction of Recording	First Mode Frequency (Hz)	Second Mode Frequency (Hz)	First Mode Damping (%)	Second Mode Damping (%)	First Mode Participation Factor	Second Mode Participation Factor	Normalized Error
Ch. 14	Ch. 2	N-S	1.801	7.909	12.16	8.06	1.681	-0.584	0.27241
Ch. 14	Ch. 3	N-S	1.765	7.617	10.40	10.70	1.531	-0.616	0.30226
Ch. 14	Ch. 4	N-S	1.785	6.579	11.02	7.99	1.097	0.127	0.28329
Ch. 14	Ch. 5	N-S	1.766	6.456	11.50	6.13	1.119	0.111	0.28968
Ch. 14	Ch. 6	N-S	1.755	6.387	11.62	4.82	1.204	0.204	0.32103
Ch. 14	Ch. 7	N-S	1.762	7.358	9.16	12.51	0.355	0.637	0.16875
Ch. 14	Ch. 8	N-S	1.756	6.797	14.22	26.64	0.550	0.819	0.18982
Ch. 14	Ch. 9	N-S	1.756	6.727	16.65	21.67	0.657	1.136	0.25853
Ch. 16	Ch. 10	E-W	1.673	7.441	6.40	9.19	1.527	-0.674	0.10141
Ch. 16	Ch. 11	E-W	1.674	7.429	6.14	9.46	1.042	0.171	0.092539
Ch. 16	Ch. 12	E-W	1.669	7.354	5.45	8.12	0.362	0.600	0.094789

Table 7. Results of the modal parameters identification of a 10-story building in Burbank for two components of an earthquake.

System Inputs	System output	Direction of Recording	Mode No.	Frequency (Hz)	Damping (%)	c_{xx} or c_{yy}	c_{xy} or c_{yx}	Normalized Error
Channel 14 & 16	Ch. 2	N-S	1	1.800	11.77	1.664	0.135	0.26982
			2	7.915	8.10	-0.605	0.0319	
Channel 14 & 16	Ch. 3	N-S	1	1.765	10.07	1.516	0.102	0.30043
			2	7.613	11.09	-0.628	-0.0344	
Channel 14 & 16	Ch. 4	N-S	1	1.785	10.82	1.092	0.0557	0.28208
			2	6.571	8.05	0.120	0.0171	
Channel 14 & 16	Ch. 5	N-S	1	1.767	11.06	1.105	0.0887	0.28681
			2	6.473	5.62	0.103	-4.581E-3	
Channel 14 & 16	Ch. 6	N-S	1	1.756	11.08	1.182	0.103	0.31647
			2	6.412	4.38	0.199	-0.0288	
Channel 14 & 16	Ch. 7	N-S	1	1.762	8.94	0.353	0.0227	0.16838
			2	7.363	12.44	0.634	-3.325E-3	
Channel 14 & 16	Ch. 8	N-S	1	1.757	13.84	0.545	0.0316	0.18911
			2	6.809	26.55	0.809	0.0174	
Channel 14 & 16	Ch. 9	N-S	1	1.757	16.10	0.647	0.0323	0.25771
			2	6.731	21.40	1.131	-0.0354	
Channel 14 & 16	Ch. 10	E-W	1	1.672	6.36	1.524	-0.0370	0.10015
			2	7.442	8.91	-0.660	-0.0311	
Channel 14 & 16	Ch. 11	E-W	1	1.673	6.12	1.040	-5.710E-3	0.09233
			2	7.441	9.18	0.167	0.0111	
Channel 14 & 16	Ch. 12	E-W	1	1.669	5.42	0.360	-0.001	0.094484
			2	7.359	8.01	0.593	0.0186	

Table 8. Results of the modal parameters identification of a 10-story building in Burbank for three components of an earthquake.

System Inputs	System output	Direction of Recording	Mode No.	Frequency (Hz)	Damping (%)	c_{xx} or c_{yy}	c_{xy} or c_{yx}	c_{xz} or c_{yz}	Normalized Error
Ch. 14,15&16	Ch. 2	N-S	1	1.798	11.67	1.668	0.132	0.168	0.26768
			2	7.928	8.13	-0.617	0.0276	0.0636	
Ch. 14,15&16	Ch. 3	N-S	1	1.765	10.07	1.517	0.0999	0.0117	0.30003
			2	7.599	11.90	-0.625	-0.0368	-0.0880	
Ch. 14,15&16	Ch. 4	N-S	1	1.784	10.78	1.097	0.0544	0.0917	0.28034
			2	6.554	8.11	0.121	0.0175	0.0415	
Ch. 14,15&16	Ch. 5	N-S	1	1.767	11.06	1.107	0.0881	0.0410	0.28637
			2	6.464	5.78	0.105	-2.906E-3	0.0243	
Ch. 14,15&16	Ch. 6	N-S	1	1.756	11.07	1.182	0.102	0.0248	0.31637
			2	6.414	4.36	0.198	-0.0294	-1.557E-3	
Ch. 14,15&16	Ch. 7	N-S	1	1.762	8.94	0.354	0.0215	0.0240	0.16817
			2	7.361	12.40	0.633	-4.659E-3	4.149E-3	
Ch. 14,15&16	Ch. 8	N-S	1	1.756	13.82	0.550	0.0396	0.0555	0.18405
			2	6.770	26.26	0.798	0.0210	0.199	
Ch. 14,15&16	Ch. 9	N-S	1	1.756	16.12	0.656	0.0460	0.0754	0.25033
			2	6.715	21.18	1.126	-0.0270	0.281	
Ch. 14,15&16	Ch. 10	E-W	1	1.671	6.41	1.520	-0.0406	0.0558	0.097404
			2	7.405	8.74	-0.658	-0.0396	-0.132	
Ch. 14,15&16	Ch. 11	E-W	1	1.672	6.20	1.040	-7.326E-3	0.0349	0.091554
			2	7.422	8.98	0.163	0.0103	0.0143	
Ch. 14,15&16	Ch. 12	E-W	1	1.669	5.49	0.363	-2.656E-4	3.694E-3	0.090238
			2	7.330	7.82	0.588	0.0260	0.111	

Table 9. Results of the modal parameters identification of a 10-story building in Burbank for four components of an earthquake.

System Inputs	System output	Direction of Recording	Mode No.	Frequency (Hz)	Damping (%)	c_{xx} or c_{yy}	c_{xy} or c_{yx}	c_{xz} or c_{yz}	c_{xr_z} or c_{yr_z}	Normalized Error
Ch. 14, 15,16, r_z	Ch. 2	N-S	1	1.788	11.16	1.632	0.122	0.150	6.389	0.26461
			2	7.759	7.45	-0.657	0.0447	0.0456	-3.455	
Ch. 14, 15,16, r_z	Ch. 3	N-S	1	1.792	11.60	1.628	0.122	0.0664	-18.509	0.26909
			2	7.734	13.24	-0.344	-0.170	-0.0595	13.028	
Ch. 14, 15,16, r_z	Ch. 4	N-S	1	1.787	11.02	1.112	0.0553	0.0974	-1.433	0.27922
			2	6. 479	8.51	0.133	5.877E-3	0.0491	1.709	
Ch. 14, 15,16, r_z	Ch. 5	N-S	1	1.781	11.57	1.110	0.0976	0.0616	-7.155	0.27991
			2	6.496	8.35	0.138	-0.0204	0.0252	-0.158	
Ch. 14, 15,16, r_z	Ch. 6	N-S	1	1.776	11.44	1.149	0.123	0.0527	-10.891	0.29164
			2	6.481	5.85	0.210	-0.0321	-0.0224	-3.955	
Ch. 14, 15,16, r_z	Ch. 7	N-S	1	1.803	11.00	0.388	0.0260	0.0491	-7.189	0.15507
			2	7.262	13.18	0.726	-0.0474	6.503E-3	3.785	
Ch. 14, 15,16, r_z	Ch. 8	N-S	1	1.739	11.00	0.467	0.0527	0.147	4.176	0.15037
			2	7.019	23.07	0.639	0.0796	0.0552	-10.330	
Ch. 14, 15,16, r_z	Ch. 9	N-S	1	1.750	11.24	0.486	0.0673	0.199	2.208	0.16837
			2	6.974	21.44	0.995	0.0485	0.0576	-19.417	
Ch. 14, 15,16, r_z	Ch. 10	E-W	1	1.671	6.43	1.523	-0.0438	0.0558	-1.183	0.097204
			2	7.402	8.77	-0.665	-0.0341	-0.135	0.0823	
Ch. 14, 15,16, r_z	Ch. 11	E-W	1	1.672	6.20	1.040	-7.404E-3	0.0350	0.0488	0.09155
			2	7.416	8.96	0.163	9.318E-3	0.0151	-0.0568	
Ch. 14, 15,16, r_z	Ch. 12	E-W	1	1.668	5.46	0.361	-1.952E-3	4.716E-3	0.260	0.089832
			2	7.319	7.81	0.591	0.0152	0.115	-0.592	

frequencies, and first and second damping ratios are plotted in Figure (13) with respect to output channel number and number of input components.

In the multi-input/single-output procedure explained, for each output channel, different values may be obtained for modal frequencies and damping ratios. For a unique value assignment for these parameters for each direction, mean values of the computed parameters are shown in Table (10). Also, in order to estimate dispersion of the modal frequencies and modal damping ratios, coefficients of variation of these parameters were also computed and are given in the Table (10). Coefficients of variation of parameters were computed using division of the standard deviation of parameters by their mean values expressed in percent [26]. Also, the mean value of normalized errors and coefficient of variation of these parameters are included in Table (10) for different input components. From the results of Table (10), it can be concluded that:

- Considerable difference exists between the

Table 10. Mean values and coefficients of variations of modal frequencies, modal damping ratios and normalized errors in the N-S and E-W directions with respect to the number of input components.

Direction	Mode No.	Number of Inputs of Dynamic System	Mean Value of Frequency (Hz)	Coefficient of Variation of Frequency (%)	Mean Value of Damping (%)	Coefficient of Variation of Damping (%)	Mean Value of Normalized Error	Coefficient of Variation of Normalized Error (%)
N-S	1	1	1.768	0.93	12.09	19.40	0.2607	20.68
		2	1.769	0.89	11.71	19.31	0.2589	20.39
		3	1.768	0.87	11.69	19.39	0.2567	20.92
		4	1.777	1.23	11.25	2.25	0.2323	26.82
	2	1	6. 979	8.21	12.32	63.37	0.2607	20.68
		2	6. 986	8.13	12.20	64.27	0.2589	20.39
		3	6. 976	8.23	12.14	63.50	0.2567	20.92
		4	7.026	7.56	12.64	51.39	0.2323	26.82
E-W	1	1	1.672	0.16	6.00	8.18	0.0962	4.78
		2	1.671	0.13	5.97	8.17	0.0957	4.18
		3	1.671	0.09	6.03	7.99	0.0931	4.08
		4	1.670	0.13	6.03	8.41	0.0929	4.20
	2	1	7.408	0.64	8.92	7.95	0.0962	4.78
		2	7.414	0.64	8.70	7.05	0.0957	4.18
		3	7.386	0.66	8.51	7.19	0.0931	4.08
		5	7.379	0.71	8.51	7.25	0.0929	4.20

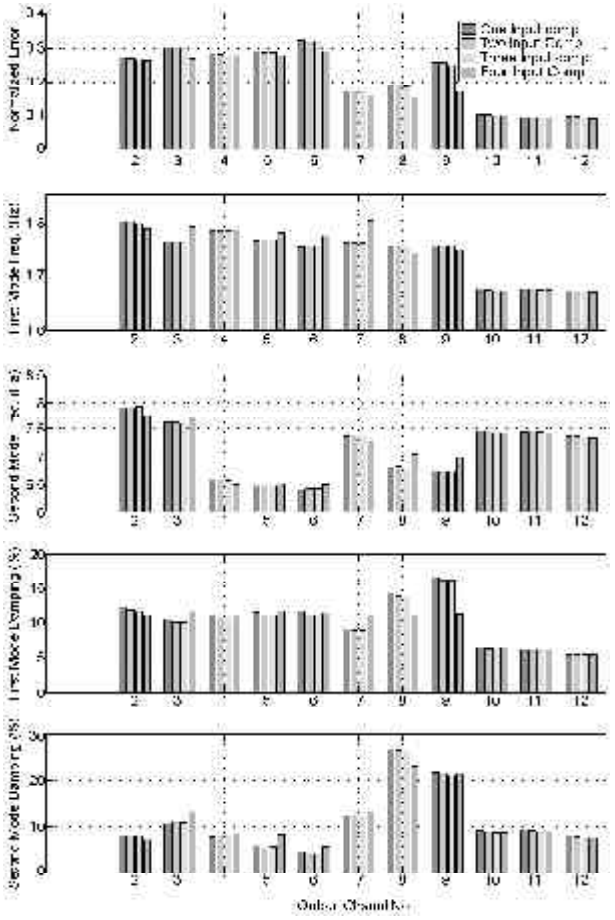

Figure 13. Variation of normalized error, 1st and 2nd modal frequencies, 1st and 2nd modal damping ratio according to channel and number of input components.

mean values of normalized errors in *N-S* direction and *E-W* direction in all cases. The mean value of normalized errors in *N-S* direction is approximately 2.5 times that of the *E-W* direction for different values of input number. Also, coefficients of variation of normalized errors in *N-S* direction in all cases are several times of those of the *E-W* direction. It is noted that the the *N-S* direction sensors are located near east and west sides of building, far from center of mass of the floors. Thus, the torsional component of the earthquake may have affected these sensors and be a cause of this considerable difference.

- The negligible decrease of mean value of normalized errors with the addition of different components of an earthquake occurred due to plan symmetry. The only exception is in the *N-S* direction, where a considerable decrease in the mean value of normalized errors occurs with the addition of the torsional component of an earthquake. This shows a noticeable effect of the torsional component on base acceleration.
- Coefficients of variation of the first and second modal frequency for both the *N-S* and *E-W* direction are always less than the coefficient of variation of corresponding modal damping

ratios for all cases. This indicates the high precision of frequencies estimates relative to damping ratios estimates.

- Coefficients of variation of the frequencies and damping ratios of the first and second modes in the *N-S* direction are greater than those of the corresponding parameters in the *E-W* direction for almost all cases. In other words, the modal frequencies and modal damping in the *N-S* direction were identified with less precision relative to the corresponding parameters in the *E-W* direction. This can be due to the *N-S* direction sensors being located far from center of mass of the floors and affected by the torsional response of building, in contrast to the *E-W* direction sensors.
- Table (10) shows a sudden decrease of the coefficient of variation of the first mode damping ratio in *N-S* direction from 19.39% for three input components to 2.25% for four input components. In contrast to other components of earthquake, the torsional component has a marked effect on the coefficient of variation of the first modal damping ratio. By including this component, the first modal damping ratios in the *N-S* direction obtained from different sensors locations reach nearly a unique value and the precision of estimation increases.

As mentioned in section 5.1 and in order to show the importance of including the torsional component of earthquake, the two additional pairs of input situations of (*x* or *y*, *z*) and (*x* or *y*, *torsion*) have been added. The results of the identification of these two additional pairs are presented in Tables (11) and (12) respectively. Mean values and coefficients of variations of modal frequencies, modal damping ratios and normalized errors in the *N-S* and *E-W* directions for three paired inputs (*x*, *y*), (*y*, *x*), (*x* or *y*, *z*) and (*x* or *y*, *torsion*) are given in Table (13) with their corresponding one input cases as base points. The following results can be extracted from Table (13):

- For the *N-S* direction, from three paired inputs (*y*, *x*), (*y*, *z*) and (*y*, *torsion*), the mean value of normalized error of (*y*, *torsion*) is less than the two other pairs. This shows the higher effect of torsional base acceleration in comparison with *E-W* and vertical base accelerations. The mean value of normalized error for the paired input (*y*, *torsion*) decreased 9.09% relative to one input situation, but, the decrease for paired inputs (*y*, *x*) and (*y*, *z*) are 0.69% and 0.61%, respectively, which is negligible.
- For *E-W* direction, where accelerographs were installed about the center of the floors, this is not true. In this direction, the mean values of the normalized errors for the paired input (*x*, *y*) and (*x*, *torsion*) did not change considerably. The mean value of the normalized

Table 11. Results of the modal parameters identification of a 10-story building in Burbank for (*x* or *y*, *z*) components of an earthquake.

System Inputs	System Output	Direction of Recording	Mode No.	Frequency (Hz)	Damping (%)	c_{xx} or c_{yy}	c_{xz} or c_{yz}	Normalized Error
Channel 14 & 15	Ch. 2	N-S	1	1.799	12.03	1.685	0.175	0.27015
			2	7.925	8.09	-0.598	0.0599	
Channel 14 & 15	Ch. 3	N-S	1	1.765	10.39	1.532	0.0129	0.30182
			2	7.601	10.47	-0.612	-0.0904	
Channel 14 & 15	Ch. 4	N-S	1	1.784	10.96	1.101	0.0967	0.28148
			2	6.574	7.98	0.127	0.0317	
Channel 14 & 15	Ch. 5	N-S	1	1.766	11.48	1.122	0.0449	0.28917
			2	6.449	6.22	0.113	0.0253	
Channel 14 & 15	Ch. 6	N-S	1	1.753	11.62	1.206	0.0268	0.32086
			2	6.383	4.84	0.206	0.0175	
Channel 14 & 15	Ch. 7	N-S	1	1.762	9.15	0.356	0.0254	0.16852
			2	7.356	12.48	0.635	3.470E-3	
Channel 14 & 15	Ch. 8	N-S	1	1.757	13.83	0.545	0.0316	0.18911
			2	6.809	26.57	0.809	0.0174	
Channel 14 & 15	Ch. 9	N-S	1	1.754	16.86	0.668	0.0713	0.2514
			2	6.706	21.32	1.130	0.278	
Channel 14 & 15	Ch. 10	E-W	1	1.672	6.44	1.523	0.0478	0.098986
			2	7.401	9.02	-0.670	-0.129	
Channel 14 & 15	Ch. 11	E-W	1	1.673	6.22	1.043	0.0340	0.091806
			2	7.414	9.36	0.168	0.0131	
Channel 14 & 15	Ch. 12	E-W	1	1.669	5.53	0.365	4.413E-3	0.090823
			2	7.324	8.02	0.598	0.108	

Table 12. Results of the modal parameters identification of a 10-story building in Burbank for (*x* or *y*, *torsion*) components of an earthquake.

System Inputs	System Output	Direction of Recording	Mode No.	Frequency (Hz)	Damping (%)	c_{xx} or c_{yy}	c_{xr_z} or c_{yr_z}	Normalized Error
Channel 14 & r_z	Ch. 2	N-S	1	1.791	11.59	1.642	6.141	0.26876
			2	7.703	7.12	-0.616	-3.902	
Channel 14 & r_z	Ch. 3	N-S	1	1.786	11.78	1.637	-14.241	0.27517
			2	7.799	14.35	-0.416	13.618	
Channel 14 & r_z	Ch. 4	N-S	1	1.788	11.25	1.113	-1.077	0.28224
			2	6.516	8.75	0.141	1.609	
Channel 14 & r_z	Ch. 5	N-S	1	1.779	11.97	1.121	-6.166	0.28444
			2	6.469	8.92	0.141	-0.466	
Channel 14 & r_z	Ch. 6	N-S	1	1.773	11.94	1.166	-9.563	0.29762
			2	6.452	6.29	0.219	-4.435	
Channel 14 & r_z	Ch. 7	N-S	1	1.799	11.08	0.388	-6.065	0.15749
			2	7.238	13.34	0.711	3.638	
Channel 14 & r_z	Ch. 8	N-S	1	1.746	11.84	0.473	2.400	0.15674
			2	7.026	24.93	0.720	-10.393	
Channel 14 & r_z	Ch. 9	N-S	1	1.753	12.06	0.491	1.128	0.17378
			2	6.977	22.29	1.048	-19.735	
Channel 16 & r_z	Ch. 10	E-W	1	1.673	6.39	1.529	-0.356	0.10136
			2	7.435	9.09	-0.670	0.299	
Channel 16 & r_z	Ch. 11	E-W	1	1.673	6.13	1.041	0.287	0.092497
			2	7.427	9.49	0.173	-0.0763	
Channel 16 & r_z	Ch. 12	E-W	1	1.669	5.42	0.360	0.175	0.094476
			2	7.348	8.06	0.599	-0.466	

Table 13. Mean values and coefficients of variations of modal frequencies, modal damping ratios and normalized errors in the N-S and E-W directions for one input and different combination of paired input situations.

Direction	Mode No.	Direction of Inputs of Dynamic System	Mean Value of Frequency (Hz)	Coefficient of Variation of Frequency (%)	Mean Value of Damping (%)	Coefficient of Variation of Damping (%)	Mean Value of Normalized Error	Coefficient of Variation of Normalized Error (%)
N-S	1	*y*	1.768	0.93	12.09	19.40	0.2607	20.68
		(*y* , *x*)	1.769	0.89	11.71	19.31	0.2589	20.39
		(*y* , *z*)	1.768	0.91	12.04	19.65	0.2591	20.80
		(*y*, *torsion*)	1.777	1.05	11.69	3.04	0.2370	26.30
	2	*y*	6. 979	8.21	12.32	63.37	0.2607	20.68
		(*y* , *x*)	6. 986	8.13	12.20	64.27	0.2589	20.39
		(*y* , *z*)	6. 975	8.27	12.25	63.05	0.2591	20.80
		(*y*, *torsion*)	7.023	7.62	13.25	52.94	0.2370	26.30
E-W	1	*x*	1.672	0.16	6.00	8.18	0.0962	4.78
		(*x* , *y*)	1.671	0.13	5.97	8.17	0.0957	4.18
		(*x* , *z*)	1.671	0.12	6.06	7.83	0.0939	4.75
		(*x*, *torsion*)	1.672	0.14	5.98	8.40	0.0961	4.84
	2	*x*	7.408	0.64	8.92	7.95	0.0962	4.78
		(*x* , *y*)	7.414	0.64	8.70	7.05	0.0957	4.18
		(*x* , *z*)	7.380	0.66	8.80	7.92	0.0939	4.75
		(*x*, *torsion*)	7.403	0.65	8.88	8.31	0.0961	4.84

paired inputs decreased 0.52% and 0.10%, respectively relative to the one input case, which is negligible. Note the considerable effect of the vertical component of base acceleration where the decrease in the mean value of normalized error for paired input (*x*, *z*) is 2.39%. This value is not high, but is more than the effect of horizontal and torsional components of earthquake.

- The coefficient of variation of the first mode in the *N-S* direction has an abrupt decrease for paired input (*y*, *torsion*). The coefficient of variation of this parameter decreased from 19.40% for the *y* input to 3.04% for paired input (*y*, *torsion*). This represents the strong effect of torsional base acceleration component in the identification of the first mode damping ratio in *N-S* direction in comparison with other base acceleration components. This was also previously observed for the cumulative effect of base acceleration components.

6. Conclusions

By presenting a multi-input/single-output modal identification method for linear systems and with the analysis of artificial and real acceleration records, the following conclusions can be made:

- The proposed method can include the effects of different components of the earthquake for the identification of modal parameters. By including these effects, modal parameters specially modal damping ratios, can be identified more precisely. Also, the compatibility between the assumed response model and the measured response of a structure increases by including these effects.
- Analyzing the seismic response of a symmetric 10-story building during the Northridge earthquake indicated that the torsional component of an earthquake effects on the identification of the first mode damping ratio parameter. The seismic response of more buildings must be analyzed to confirm this.
- The output-error method identifies the parameters of a class of models assumed at the first stage of identification process; i.e. linear models with classical damping. Therefore, from a global point of view, it is necessary to examine the other class of models such as linear models with non-classical damping, bi-linear models and other nonlinear models and so on. Finally, by considering all the probable class of models, the most appropriate one should be chosen.

References

1. Beck, J.L. (1978). "Determining Models of Structures from Earthquake Records", EERL 78-01, Earthquake Engineering Research Laboratory, California Institute of Technology, Pasadena, California.

2. Peng, C. (1987). "Generalized Modal Identification of Linear and Nonlinear Dynamic Systems", EERL 87-05, Earthquake Engineering Research Laboratory, California Institute of Technology, Pasadena, California.

3. McVerry, GH. (1979). "Frequency Domain Identification of Structural Models from Earthquake Records", EERL 79-02, Earthquake Engineering Research Laboratory, California Institute of Technology, Pasadena, California.

4. Li, Y. and Mau, S.T. (1991). "A Case Study of MIMO Identification Applied to Building Seismic Records", *Earthquake Engineering and Structural Dynamics*, **20**, 1045-1064.

5. Goel, R.K. and Chopra, A.K. (1997). "Vibration Properties of Buildings Determined from Recorded Earthquake Motions", *Earthquake Engineering Research Center*, Report No. UCB/EERC-97/14, University of California at Berkeley.

6. Ljung, L. (1995). "System Identification TOOLBOX User's Guide: For Use with MATLAB", The Math Works Inc.

7. Arici, Y. and Mosalam, KM. (2003). "System Identification of Instrumented Bridge Systems", *Earthquake Engineering and Structural Dynamics*, **32**, 999-1020.

8. Aghakochak, A.A. and Memari, A.M. (1994). "Forced and Ambient Vibration Tests on Real Buildings", IIEES Report No. 72-94-2, International Institute of Earthquake Engineering and Seismology, Tehran, Iran (In Farsi).

9. Memari, A.M., Yazdani Motlagh, A.R., Akhtari, M., Scanlon, A., and Ghafory-Ashtiany, M. (1999). "Seismic Vulnerability Evaluation of a 32-Story Reinforced Concrete Building", *Journal of Structural Engineering and Mechanics*, **7**(1), 1-18.

10. Ghafory-Ashtiany, M., Kazem, H., and Tiv, M. (1998). "Forced Vibration Test of 1:2 Scaled Model of a 4-Story Steel Structure", Report No. 77-98-11, International Institute of Earthquake Engineering and Seismology, Tehran, Iran (In Farsi).

11. Ghafory-Ashtiany, M., Tiv, M., Mahmoudabadi, M., and Tehranizadeh, M, (1996). "Parameter Identification of Jack-Arch Masonry Floors using Forced Vibration Test of 1/2 Scaled Model of a 4-Storey Steel Structure", *Proceedings of Eleventh World Conference on Earthquake Engineering*, Paper No. 1365, Acapulco, Mexico.

12. Kazem, H., Ghafory-Ashtiany, M., and Tehranizadeh, M. (1998). "Dynamic

Characteristics of Khorjini Semi-Rigid Connections, using Forced Vibration Test of 1/2-Scaled Model of a 4-Story Steel Structure", *Proceedings of the Eleventh European Conf. on Earthquake Engineering*, Paris-France.

13. Saberi-Haghighi, K., Ghafory-Ashtiany, M., and Lucas, C (2000). "Damage Assessment Using Neural Network and Genetic Algorithm", *Journal of Seismology and Earthquake Engineering*, **2**(2), 29-43.

14. Ghafooripour, A. and Aghakoochak, A. (2003). "Evaluation of Dynamic Behavior of an Offshore Structure Using Non-Stationary Spectral Analysis with Bessel-Kaiser Window Function", *Proceedings of the Fourth International Conference on Seismology and Earthquake Engineering*, Tehran, Iran.

15. Mivehchi, M.R. (2001). "Evaluation of Discrepancies Between the Dynamic Characteristics of Mathematical and Prototype Models of a Concrete Arch Dam; Some Proposed Modifications in Mathematical Models", PhD Dissertation, Dept. of Science and Research, Islamic Azad University, Tehran, Iran (In Persian).

16. Davoodi, M. (2003). "Evaluation of Dynamic Characteristics of Embankment Dams Using Ambient and Forced Vibration Tests", PhD Dissertation, International Institute of Earthquake Engineering and Seismology, Tehran, Iran (In Persian).

17. Werner, S.D., Beck, J.L., and Levine, M.B. (1987). "Seismic Response Evaluation of Meloland Road Overpass Using 1979 Imperial Valley Earthquake Records", *Earthquake Engineering and Structural Dynamics*, **15**, 249-274.

18. Hanselman, D. and Littlefield, B. (1995). Mastering MATLAB, A Comprehensive Tutorial and Reference, Prentice-Hall.

19. MATLAB Reference Guide: High Performance Numeric Computation and Visualization Software, (1992). The Math Works Inc., MA.

20. Grace, A. (1994). "Optimization TOOLBOX User's Guide: For Use with MATLAB", The Math Works Inc, MA.

21. Kraus, T.P., Shure, L., and Little, J.N. (1994). "Signal Processing TOOLBOX User's Guide: For Use with MATLAB", The Math Works Inc., MA.

22. Chopra, A.K. (2001). "Dynamics of Structures-Theory and Applications to Earthquake Engineering", 2nd Ed., Prentice-Hall.

23. Mahmoudabadi, M. (2005). "Modal Identification of Instrumented Buildings under Multi-Component Earthquake", PhD Dissertation International Institute of Earthquake Engineering and Seismology, Tehran, Iran (In Persian).

24. Naeim, F. (1996). "Performance of Instrumented Buildings During the Jan. 17, 1994 Northridge Earthquake - An Interactive Information System-", Draft Report, California Strong Motion Instrumentation Program.

25. Limongelli, M.P. (2003). "Optimal Locations of Sensors for Reconstruction of Seismic Responses Through Spline Function Interpolation", *Earthquake Engineering and Structural Dynamics*, **32**, 1055-1074.

26. Sanders, D.H., Eng, R.J., and Murph, A.F. (1985). "Statistics, a Fresh Approach", 3rd Ed., McGraw-Hill.